Journal of Radioanalytical Chemistry, Vol. 63, No. 1. (1981) 97–119

FACILITY FOR NON-DESTRUCTIVE ANALYSIS FOR MAJOR AND TRACE ELEMENTS USING NEUTRON-CAPTURE GAMMA-RAY SPECTROMETRY

D. L. ANDERSON,* M. P. FAILEY*†, W. H. ZOLLER,* W. B. WALTERS,*
G. E. GORDON,* R. M. LINDSTROM**

**Department of Cehmistry, University of Maryland, College Park, Maryland 20742 (USA)*
***Center for Analytical Chemistry, National Bureau of Standards, Washington, D. C. 20234 (USA)*

(Received October 10, 1980)

A facility for neutron-capture γ-ray spectroscopy for analytical purposes has been developed and tested at the National Bureau of Standards reactor. The system consists of an internal beam tube with collimators, an external beam tube and irradiation station, a Compton-suppressed Ge(Li) γ-ray detection system, and a minicomputer-based data-collection and -analysis system. Detection limits have been established for many elements and errors arising from neutron self shielding, γ-ray peak overlap, neutron beam variations, and sample matrix evaluated.

Introduction

The potential for analytical use of neutron capture γ-ray spectroscopy has been recognized for some time. ISENHOUR and MORRISON[1,2] used reactor neutrons to measure concentrations of some abundant elements and DUFFEY, EL-KADY, and SENFTLE[3] explored the use of neutrons from ^{252}Cf for similar purposes. More recently, HENKELMANN and BORN[4] determined detection limits for a number of elements using only low-energy γ-rays. GLADNEY, JURNEY and CURTIS[5–8] analyzed various materials for several elements by placing samples in a thermal column and observing γ-rays outside of the shielding. GLADNEY has compiled a bibliography of 190 references to the literature of the field.[9] In most studies, experimenters have used facilities designed primarily for some other purpose, mostly for long irradiations of certain nuclides to obtain nuclear level information from neutron capture γ-ray spectra. These facilities have generally not been designed for optimum use in analytical applications.

†Present address: Babcock and Wilcox, LRC, Lynchburg, Virginia 24505.

In this paper we describe the design, construction, operating characteristics and performance of a neutron-capture γ-ray spectrometer built specifically for analytical purposes. The design goals included a low background for elements that can be observed in spectra of geological, environmental, biological and industrial samples, a sufficient flux to keep irradiation times reasonably short, and a sample-holding system versatile enough to permit the study of a wide range of samples with quick, reproducible sample positioning. We have designed and built such a system and tested it by analyzing many types of samples. Analytical results obtained with the system have been described elsewhere.[10]

To accommodate a wide variety of samples, e.g., liquids, solids, gases or hazardous materials such as fuels or explosives, and to achieve maximum flexibility in sample and detector arrangements, we chose to irradiate samples in an external beam, where few limitations exist as to the size and composition of the sample. An external beam tube of diameter much greater than that of the beam was used to minimize interactions of neutrons in the fringe of the beam with the walls. Massive amounts of polystyrene, paraffin, boron carbide (B_4C), Li_2CO_3 and Pb were used to slow down and absorb scattered neutrons, and to eliminate background γ-radiation caused by the neutron absorptions. The detection system must be capable of observing γ-rays with good resolution from about 0.1 to 11 MeV. We used a large Ge(Li) detector surrounded by a split-annulus NaI(Tℓ) crystal for obtaining singles, Compton-suppressed and pair spectra. To obtain all information from the detector system, one should have a data-acquisition system capable of accumulating up to six 8192-channel spectra with a foreground-background capability so that spectral analysis can proceed simultaneously with data collection.

Experimental

Beam handling and sample positioning

The neutron beam is extracted vertically from the National Bureau of Standards (NBS) reactor from a region in the D_2O reflector approximately 0.5 m from the nearest fuel elements. The beam thimble (in the reactor) is composed of five main sections, each containing its own series of collimating and spacing annuli. The overall configuration of the thimble is illustrated schematically in Fig. 1. The collimation annuli are constructed of materials that thermalize the fast neutrons, collimate the thermal neutrons, and attenuate the γ-rays originating in the reflector region and in the Al window at the end of the beam thimble.

The tube section labeled I is 0.32-cm wall Al tube, 4.4 m in length with a 0.16-cm Al end window. This tube extends down into the D_2O moderator to a

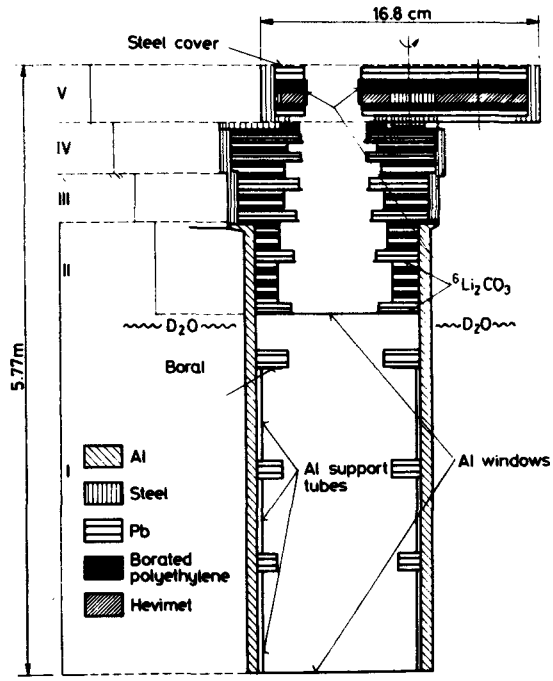

Fig. 1. Beam thimble with collimators. For clairty, the horizontal scale has been expanded by a factor of 16 relative to the vertical scale

point level with the center line of the reactor core. The thermal neutron flux at the bottom of the thimble is $3.2 \cdot 10^{13}$ n $\cdot$ cm^{-2} $\cdot$ sec^{-1}. The tube section labeled II provides a seal at the top of the first section enabling Section I to be filled with He gas. The gas fill is used because of the lower neutron scattering and capture cross sections of He as compared to those of N_2 and O_2 in air.

Section II is an Al tube 83 cm in length inserted into the upper part of Section I. At the bottom of the tube is a 0.32-cm thick Al window. Sections III and IV are constructed of stainless steel with no provision for He gas, which was not needed because of the presence of the collimators which act as scattering points for neutrons outside the collimation cone.

The final section of the thimble consists of a rotating beam shutter, the top of which is flush with the control room floor (just above the top of the reactor shielding). This apparatus contains sections of borated polyethylene, Pb and a large plug of "Hevimet" (a W alloy) which effectively shuts off the neutron and γ radiations in the beam. Surrounding the shutter, drive motor and gearing mechanism is a rectangular box filled with a mixture of natural Li_2CO_3, steel shot and paraffin which

provides shielding for radiation scattered out the sides of the beam shutter. A manual switch activates the drive motor which rotates the shutter at about 0.9 rpm. Gamma radiation above the closed beam shutter is about twice that of room background. The thermal-neutron leakage directly above the shutter is approximately $10\ n \cdot cm^{-2} \cdot s^{-1}$.

Gamma radiation collimation in the beam is accomplished primarily through the use of Pb and steel annuli. In addition, there is a 10-cm Hevimet collimator in the shutter assembly for γ-radiation collimation. Thermalization and collimation of the fast neutron component occurs primarily through inelastic collisions in the Pb and steel inserts along with elastic collisions and, finally, absorption in the borated polyethylene and $^6Li_2CO_3$-polystyrene collimators. Thermal neutron collimation is achieved using several thin, $^6Li_2CO_3$-polystyrene apertures and a single boral (Al-B_4C mixture clad in Al plate) annulus which receives most of the initially high neutron flux. With the exception of the $^6Li_2CO_3$-loaded polystrene composite, the neutron absorber materials are commercially available. Collimators of fused ^6LiF and $^6Li_2CO_3$ were considered, but found to possess insufficient mechanical strength. The material found to be most satisfactory consisted of $^6Li_2CO_3$ cast in a commercially available polystyrene-polyester resin (Clear Cast, American Handycrafts Corp.), a material which has excellent radiation-resistant properties.

The Li_2CO_3 must be dried before the resin is cast, as water or LiOH inhibits the polymerization. The maximum loading of Li_2CO_3 in the composite is equivalent to a weight ratio of Li_2CO_3/resin of about 2/3. The composite is cast in molds lined with Al foil to prevent adhesion. Polymerization occurs within 1 to 5 days after addition of the organic peroxide catalyst. The cast composite is easily machined and has withstood about two years of exposure to a neutron flux of $10^8\ n \cdot cm^{-2} \cdot sec^{-1}$ without observable damage.

The beam stop is positioned 2.1 m above the top of the reactor shielding and consists of a cube, 30 cm on a side, of molded polystyrene doped with 2% by weight natural Li_2CO_3 surrounded by Pb, which is 10 cm thick on the sides, 20 cm thick on top and 5 cm thick on the bottom. The assembly is held in place by welded steel plates and is supported by a three-legged welded-Al frame. Bolts in the legs sit upon steel floor pads. These bolts were made adjustable for fine tuning of the beam-stop alignment. The beam enters a 7.6-cm diam hole in the Li_2CO_3 cube to a depth of 10 cm, where a 2.5-cm thick $^6Li_2CO_3$-polystyrene disc absorbs most neutrons. Area radiation monitors 6 m above the beam stop register no measurable increase when the beam shutter is opened.

The external beam tube, from the shutter to the beam stop, consists of three concentric Plexiglas cylinders with outer diameters of 10.2 cm, 25.4 cm and 30.6 cm. It is contained in a wheel-mounted Al cage for easy removal. Horizontal

and vertical views of the beam tube and detector assembly are shown in Figs. 2 and 3, respectively. The inner tube is enclosed at the ends so that it can be filled with a continuously flowing inert gas such as He to reduce scattering, but the windows (0.0025-cm Teflon) are not strong enough to support a vacuum. The space between the inner and middle tube is filled with paraffin containing 1% natural Li_2CO_3 and that between the middle and outer tube is filled with B_4C in a paraffin matrix. The B_4C powder must be embedded in a matrix to prevent its leaking into the reactor. The powder is so abrasive that it could cause severe damage to the reactor parts. Most parts containing B_4C must be cast, as the B_4C particles are so hard that the material is very difficult to machine.

The hydrogen in the Plexiglas and paraffin effectively thermalizes the fast neutrons that strike the beam-tube wall. The thermalized neutrons must be captured to prevent their escape to the surroundings, which would cause hazard to personnel, high backgrounds, radiation damage and possible activation of the detector materials. There are essentially three elements that can be used effectively for capture of neutrons: Li, B and Cd. Pure ^6Li has a high cross-section[11] and the additional advantage that it yields no γ-rays upon capture, only charged particles ^4He and ^3H. However, pure ^6Li is too expensive to be used in massive amounts. Natural Li is much less effective, as it contains only 6% of ^6Li, but it can be used in large quantities. Cadmium has cross sections ranging from 2000 to 8000 b for neutrons below 0.3 eV, but at higher energies, B has higher cross sections.[11] Since the neutrons are not completely thermalized, B is on the average an equivalent or better absorbing material. Both B and Cd emit γ-rays following capture, but B yields only a low energy (478 keV) line, whereas Cd emits some high energy γ rays. Thus, we used B_4C as our major neutron-absorbing material, but natural Li_2CO_3 in some places to avoid γ-emission. Since B emits the 478-keV γ-ray upon capturing neutrons, it is necessary to have γ-absorbing material between the detection system and the B_4C.

The beam tube and stop are quite effective in containing the neutrons. With an integrated flux of $3 \cdot 10^9$ $n \cdot sec^{-1}$ in the tube, the neutron flux at the outer surface of the beam tube ranges from about 80 $n \cdot cm^{-2} \cdot sec^{-1}$ at the bottom to 20 at the top with the shutter open.

A Plexiglas sample box of outside dimensions $30 \times 30 \times 20$ cm^3 was built into the external beam tube, centered at about 110 cm above the floor. One side of the box perpendicular to the side on which the detector is located can be removed for insertion of samples. Plexiglas sample frames (15×21 cm^2) are slid into Plexiglas rails attached diagonally to the top and bottom of the box to hold samples at 45 deg with respect to the beam and to the axis of the detection system. The sample frames have 13×15 cm^2 holes cut from the center to provide good

clearance from the beam. Samples in powder, pellet, liquid, or foil form, and ranging in mass from 0.1 to 2.5 g are packaged in thin (typically 0.0025 cm) Teflon, Mylar, or polyethylene bags. The bags are held in constant position in the sample frame by sandwiching them between thin Nylon fish line and using runner knots to hold them firmly in place. Centering is achieved using a positioning template. The sample, bagging material, and runner knots are confined to the central uniform portion of the beam. Plates made of resin loaded with B_4C are attached to the outside of the sample box to absorb neutrons scattered by the target. A hole is cut out of the plate on the side opposite the detector so that the detector will not receive B lines from capture there. The volume inside the sample box is open to the inner beam tube above and below it.

Beam characteristics were measured by irradiating a Dy foil in the sample location and later exposing it to X-ray film, which was scanned with a densitometer. The major part of the beam (see Fig. 4) is about 4.5 cm in diam, with a central portion of 2-cm diam. having a uniformity of ±3%. The flux was measured by irradiating Au foils, which yielded a value of about $2 \cdot 10^8$ n $\cdot$ cm^{-2} $\cdot$ sec^{-1} in the central portion, with an integrated flux over the entire beam of $3 \cdot 10^9$ n $\cdot$ sec^{-1}. By comparing flux values obtained using Au foils with and without Cd covers, a Cd(Au) ratio of 55 was obtained.

Data collection and analysis

The data-collection and analysis system consists of a true coaxial Ge(Li) detector, a cylindrical 30×38 cm^2 split annulus NaI(Tℓ) detector and a pulse-height analyzer (PHA) system based on a minicomputer. The Ge(Li) detector has a full-width at half maximum (FWHM) of 1.85 keV for the 1332-keV γ-ray from ^{60}Co and an efficiency of 24% relative to a 7.6×7.6 cm^2 NaI detector. The detector is positioned at 90 deg with respect to the neutron beam, and surrounded by the NaI(Tℓ) annulus as shown in Figs 2 and 3.

The dimensions of the Ge(Li) crystal were chosen to ensure that about 75% of γ-rays of 10 MeV energy will interact with it in some way. The cryostat assembly was of a special design for a proper fit in the NaI(Tℓ) crystal and shielding. The Ge(Li) detector was positioned forward of the center of the NaI(Tℓ) detector to enhance absorption of the high energy Compton-scattered γ-rays at forward scattering angles. The large size of the NaI(Tℓ) crystal ensures absorption of about 80% of the scattered γ-rays of 4–10 MeV and nearly 100% of those <4 MeV.

The NaI(Tℓ) crystal has such a high counting efficiency that even under normal background conditions, the count rates would cause unacceptably high dead times in the Compton-suppression mode without good shielding. The problem is

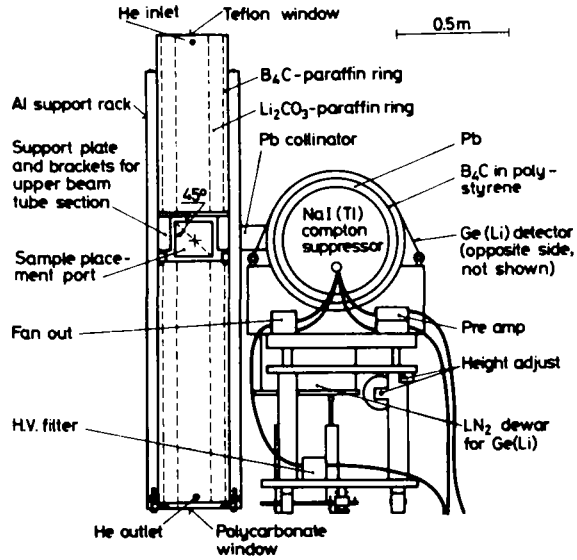

Fig. 2. Detection system and shielding configuration, horizontal view

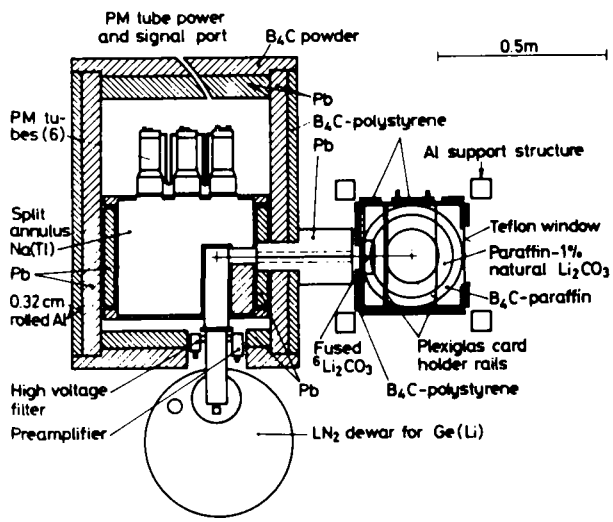

Fig. 3. Detection system and shielding configuration, vertical view

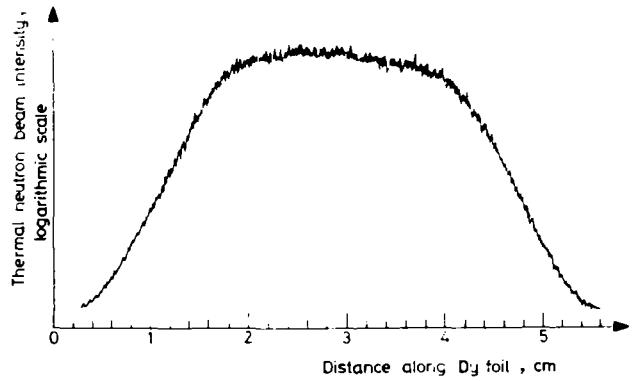

Fig. 4. Radiograph of neutron beam measured with Dy foil in the sample position and orientation

compounded by location of the detector near the beam tube in an area of elevated backgrounds. To reduce the γ-ray background to acceptable levels and to provide additional protection against neutron damage, a massive shield was designed and built around the detection system.

Diagrams of the detection system and shielding are shown in Figs 2 and 3. A cylinder of Pb 5-cm thick surrounds most of the NaI(Tℓ) crystal. This is surrounded by three concentric Al cylinders. Between the inner and middle Al cylinders is an additional 5 cm layer of Pb. The space between the middle and outer Al cylinders was filled with B_4C in polystyrene and the welded Al endcaps were filled with B_4C powder. A Pb collimator 15 cm long with a 2.5 cm inside diam was placed between the target position and the Ge(Li) detector. Initial experiments were conducted with a 2.5-cm thick, fused $^6Li_2CO_3$ plug inside the collimator to prevent neutrons scattered by the sample from striking the detector. The plug was later moved to a more accessible position just inside the sample box, where it could be removed during alignment procedures.

The data-aquisition system consists of a Tenncomp TP-5000 PHA based on a PDP 11/34 computer equipped with a 128K word memory which uses Tennecomp Interpretive Language (TIL), a language based on FOCAL. The computer controls two 2.4-megabyte disks, a 9 track magnetic tape drive, a 25 cm display screen equipped with a light pen, and up to six analog-to-digital converters (ADCs). The company-supplied search-and-fit routines served as a basis for a software package which controls both the prompt-γ setup and an off-line spectroscopy facility which runs simultaneously. A simple channel-summing and straight-line-background subtraction fitting routine was found adequate for analytical purposes, so more complex Gaussian techniques were not used.

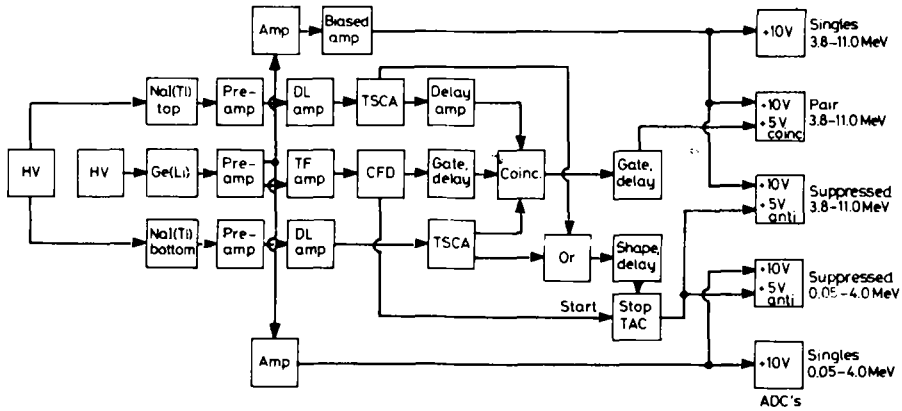

Fig. 5. Electronics block diagram for PGAA: HV – high voltage supply; DL Amp – delay-line-amplifier; TSCA – timing single-channel analyzer; CFD – constant-fraction discriminator; TAC – time-to-amplitude convertor

Up to five modes of data collection were used simultaneously. As the useful γ-rays range from 0.1 to 11.0 MeV in energy, two energy ranges were covered, one from 0.1 to 4.0 MeV, and the other, using a biased amplifier, from 3.8 to 11.0 MeV. Singles and Compton-suppressed data were collected covering both regions, while pair spectra were accumulated only in the upper range. Each of these five was fed through an 8192-channel ADC.

Fig. 5 shows the basic electronic setup for the five data accumulation modes. In the Compton-suppressed mode, all γ-ray events occurring in the Ge(Li) detector which had coincident events in the NaI(Tℓ) annulus within a specified time (50 nsec, determined by the single-channel-analyzer output of the TAC) were rejected at the two ADC inputs. For pair spectra, a triple coincidence between the Ge(Li) and the two halves of the NaI(Tℓ) crystal was required to accept a Ge(Li) pulse at the ADC. In recent experiments, a fourth coincidence requirement was added: the NaI(Tℓ) pulses derived from both halves were run through a summing amplifier and an energy gate was set spanning the 1022-keV region of the summed pulses. Adding this requirement resulted in lowering the overall background in the pair spectrum by a factor of two with no reduction in escape-peak intensities.

Absolute efficiencies for the full energy (FE), single-escape (SE) and double-escape (DE) photopeaks for the singles spectrometer and the pair spectrometer are shown in Fig. 6. The low energy points were obtained by taking spectra of an NBS γ-ray emission-rate, point-source standard, SRM 4216E, in the sample

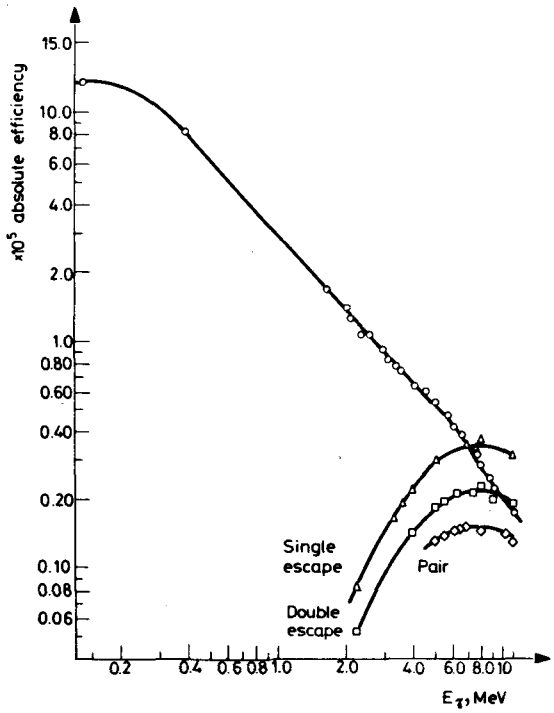

Fig. 6. Absolute efficiency curve of the detection system, which consist of a 24% efficient Ge(Li) coaxial detector (relative to 7.6 × 7.6 cm² NaI) surrounded by a 30 × 38 cm² split annulus NaI(Tℓ) crystal. The single-escape (SE) and double-escape (DE) curves are for the singles mode. SE, DE and pair data are plotted at energy of the corresponding full-energy peak

position for two hours. High energy data points were obtained from neutron-capture spectra of Fe, Al, Cl and N compounds using the energy and intensity data for the capture γ-ray lines determined by STELTS and CHRIEN.[12]

The relative efficiency of the detection system for SE and DE peaks in singles spectra is shown in Fig. 7. The results were obtained from the ratios of areas under FE, SE and DE peaks in spectra of pure elements or compounds. Since the singles, Compton-suppressed and pair spectra were taken simultaneously, one can easily make direct comparisons of corresponding peak areas in the various spectra. Because of the complex electronics for gating and timing required for the various spectra, we were concerned that there might be appreciable losses of some kinds of events. For the Compton-suppressed spectra, the intensities of the FE peaks are 98.8 ± 0.7% of their intensities in the singles

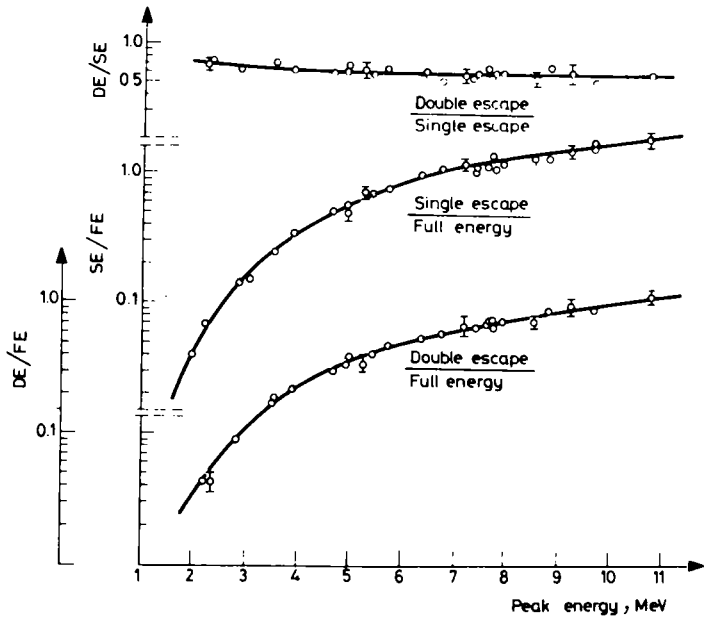

Fig. 7. Relative singles spectra efficiencies for the detection of single-and double-escape peaks with the Ge(Li) detector described in caption of Fig. 6

spectra, with no trend vs. energy from 0.3 to 8 MeV. Escape events in which annihilation photons are captured in the NaI crystal are also suppressed, so one expects much smaller SE and DE peaks in Compton-suppressed spectra. Indeed, the SE and DE efficiencies in the Compton-suppressed spectra from 4 to 9 MeV are 19.4 ± 2.3% and 7.1 ± 1.7% of the efficiencies in the singles spectrum, respectively. The SE efficiencies do not fall to zero, as the single photon may escape through the hole towards the target, along the axis of the crystal or into the 3.2 mm thick Al optical-isolation layer in the NaI detector (see Fig. 3). The 7.1% DE relative efficiency arises from the small number of events that fall outside of the 50 ns timing window and the geometrical situation in which one annihilation photon is absorbed in the optical shield in the NaI detector, and the other exits via the collimator.

Efficiencies for DE peaks in the pair spectra are 69.8 ± 1.6% of their singles-spectrum values from 4.5 to 9.5 MeV. The 30% loss of efficiency occurs because one of the two photons is not absorbed in the NaI crystal, usually because of loss out of one of the two holes in the crystal or because one photon is absorbed by the optical shield. Single-escape peaks are reduced to 4.4 ± 0.3% of their singles-spectra intensities.

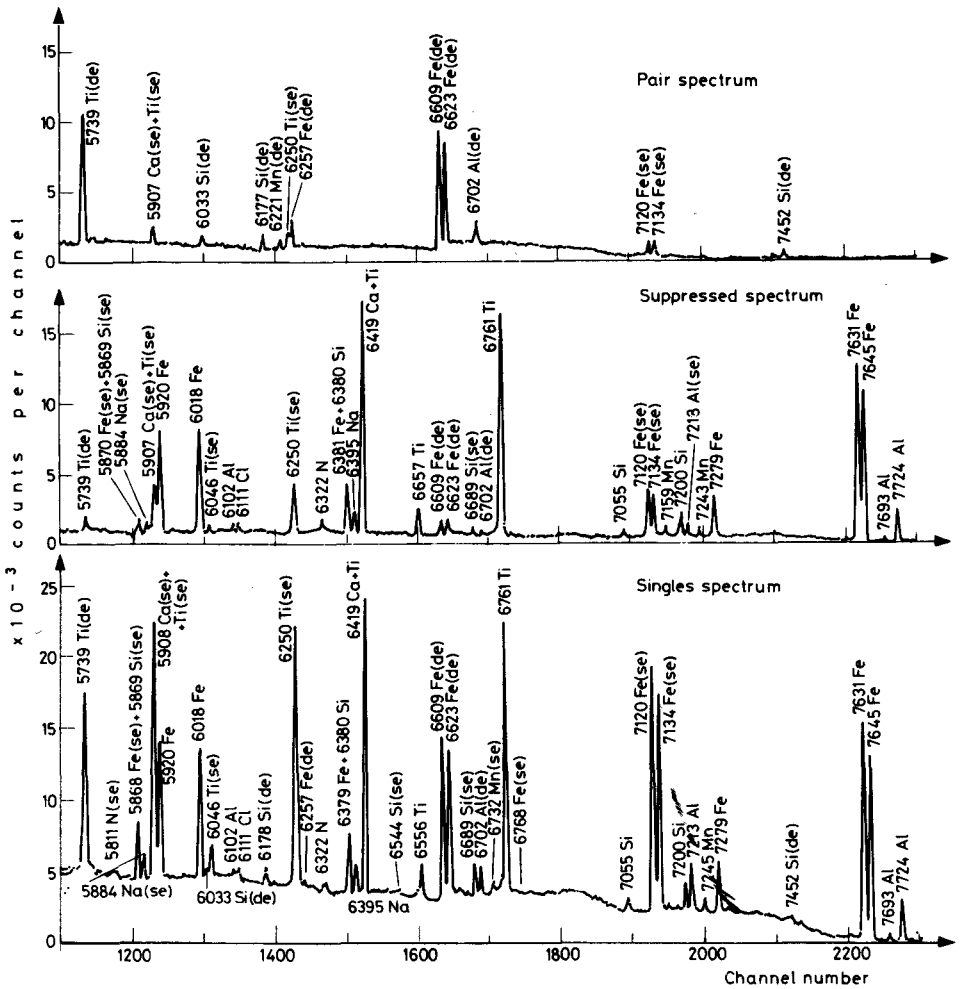

Fig. 8. Singles, Compton-suppressed and pair spectra for USGS Hawaiian Basalt BHVO-1 in the energy range 5.7 to 7.8 MeV. Peaks are identified by the symbol of the capturing element and the γ-ray energy in keV. SE and DE indicate single- and double-escape peaks, respectively

The significance of these characteristics is emphasized in Figs 8 and 9, in which we show portions of the high energy range of the three types of spectra of samples of U. S. Geological Survey (USGS) Hawaiian Basalt (BHVO-1) and Pacific Nodule (P-1), respectively. The spectra are considerably simplified by application of Compton suppression and pair requirements: in the former, SE peaks are strong-

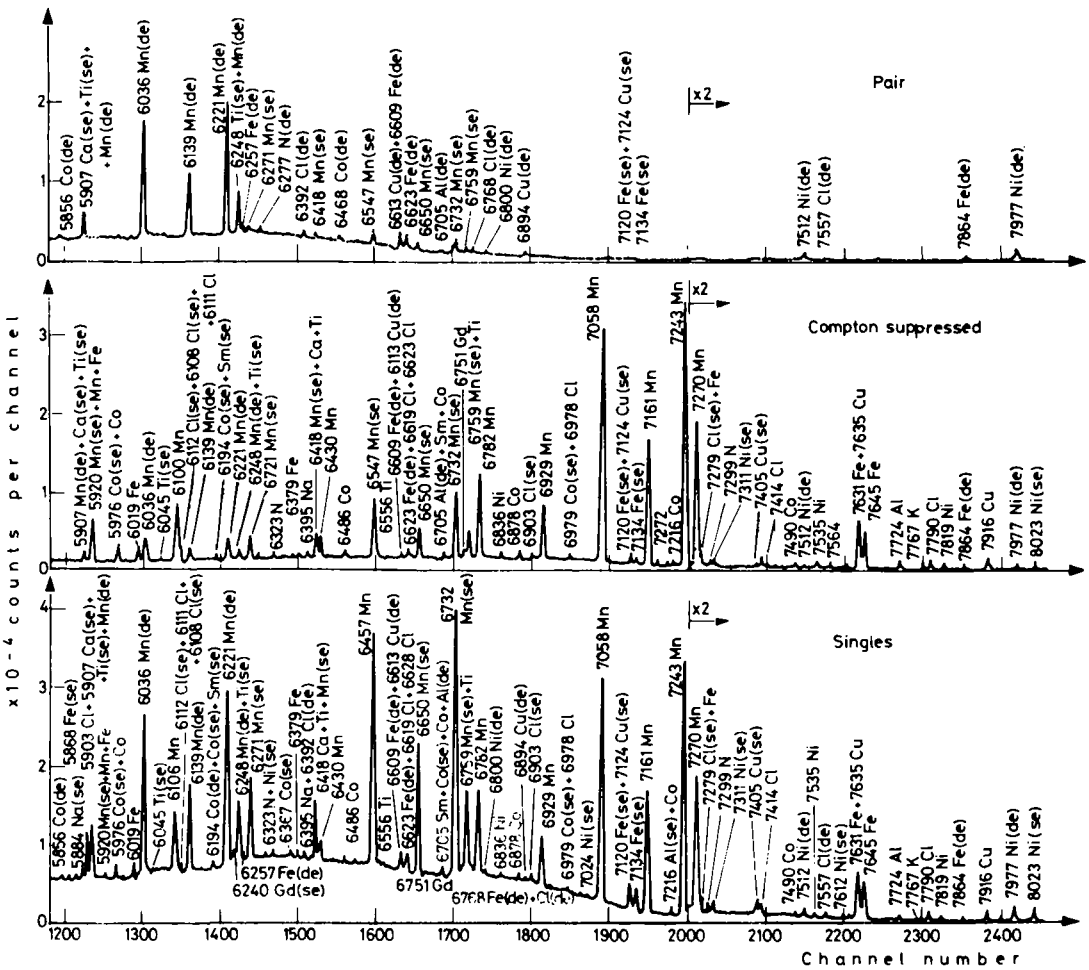

Fig. 9. Singles, Compton-suppressed and pair spectra for USGS Pacific Manganese Nodule P-1 in the energy range 5.8 to 8.0 MeV

ly reduced and DE peaks are nearly eliminated and the latter are essentially complementary, as FE peaks are totally eliminated and SE are reduced strongly. By comparison of these spectra, one can clearly identify which peaks are FE, SE and DE, and which contain an unresolved mixture of these. For example, the Fe(SE) 6768 keV line is removed from the doublet with the Ti 6761-keV line in the Compton-suppressed spectrum, and both are absent from the pair spectrum.

The general background under peaks that arises mainly from Compton events is reduced by factors of about three to five in the Compton-suppressed spectra of

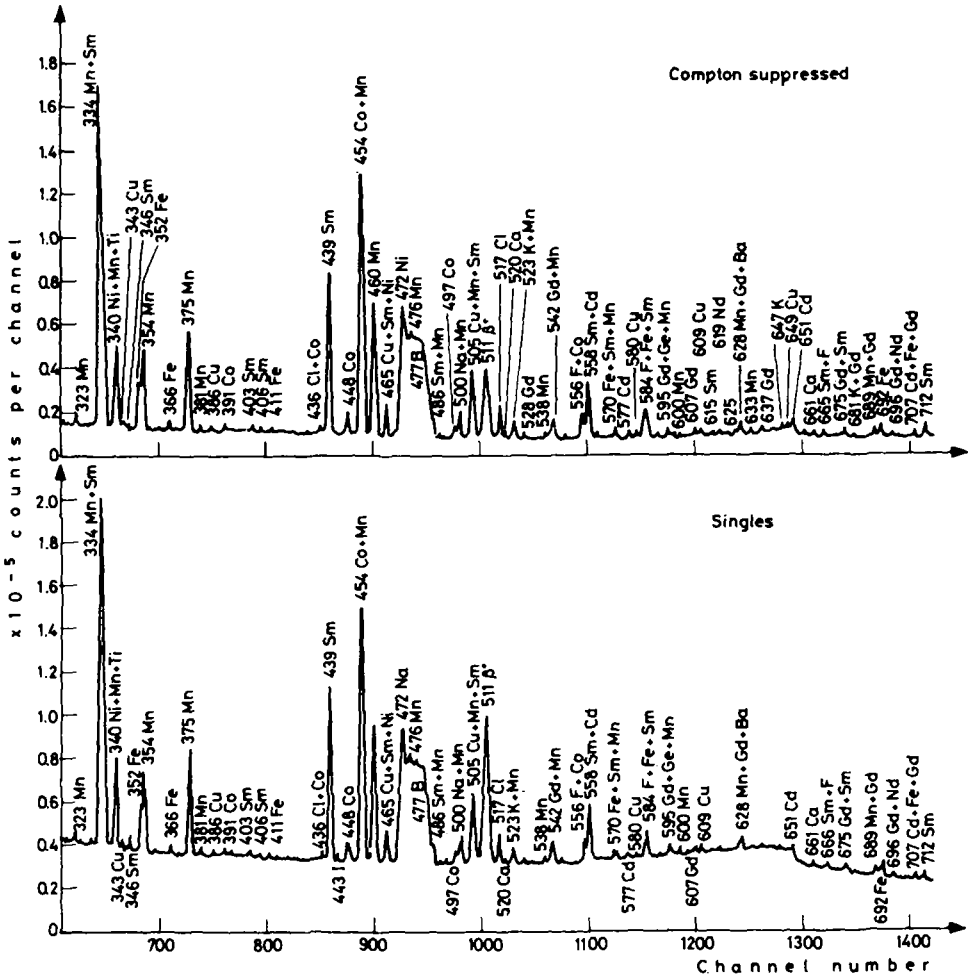

Fig. 10. Singles and Compton-suppressed spectra of USGS Pacific Manganese Nodule P-1 in the energy range of 300–730 keV

Figs 8 and 9. Although pair spectra are not very useful at low energy, Compton suppression is useful well below 1 MeV, as in the low energy spectra of the Pacific Nodule in Fig. 10. It is not possible to show a plot of the suppression ratio (background level in the singles spectrum divided by the level in the Compton-suppressed spectrum) for the system, as the ratio at a given energy depends on the features of the particular spectrum. The suppression ratio is smallest at low energies, as few Compton-scattered γ-rays escape from the large Ge crystal. Above about

500 keV, the ratio varies from about three to six, undergoing some fluctuations near large peaks.

As shown in Figs 8 to 10, the lowered general background under peaks reduces the background that must be subtracted to determine net peak areas, although we have seen very few new peaks emerge above the reduced background. The background reduction has the quantitative effect of reducing the statistical uncertainties attached to the net peak area. This improves the precision of determination of concentrations and lowers the limits of detectability of species for which only weak lines above background can be used, e.g., the Cd lines at 558 and 651 keV (see below). However, much stronger lines relative to background are known for most observable elements, so one should not overestimate the value of Compton suppression for routine analyses as distinct from research on the method. With the very large Ge(Li) detectors that are now available, the losses of Compton-scattered γ-rays from the detector have been much reduced. For our detector, the peak/Compton ratio of the detector itself is 58 at 1333 keV, and Compton suppression gains an additional factor of about three. The large NaI crystal makes it physically impossible to move the Ge(Li) detector close to the samples to increase counting efficiency. In many routine applications, the latter may be more important than reduction of Compton backgrounds.

Operation and performance

Concentrations of an element in samples are determined by comparing areas of peaks in the spectrum of the sample to those of several corresponding peaks in the spectrum of a standard containing a known quantity of the element. Although the power level of the reactor remains nearly constant for up to several weeks, one must frequently check for any changes in neutron flux in the beam and efficiency of the detection system. This is done by taking 15 min spectra of a Cr standard between taking sample spectra. Two intense γ-ray peaks at 749 and 835 keV were used routinely to detect flux and efficiency variations. Such variations over a 30-day period are shown in Table 1. Minor variations over long periods are apparently due to changing conditions of the Cd shim control rods and the nearby boron shield for the reactor's thermal column facility. As our facility is located on top of the reactor, we must periodically disassemble and move the entire detector system when fuel elements are changed. Due to the size and bulk of the apparatus, it is impossible to reproduce the geometries exactly when the system is reassembled. We typically find variations of about 5% of the system efficiency from one set-up period to another. However, count rates of the Cr standard can be used accurately to intercompare samples and standards taken at different times.

Table 1
Observed flux factor variations during one fuel cycle

Operation period, day	Normalized flux factor
(Reactor start-up)	
1 – 3	1.000
4	0.999 ± 0.001
5 – 7	0.992 ± 0.002
8 – 9	1.022 ± 0.005
10	1.017 ± 0.011
11 –11.5	1.009 ± 0.001
11.5–16.5	1.004 ± 0.007
16.5–17	1.025 ± 0.008
18 –21	1.034 ± 0.003
22 –24.5	1.027 ± 0.010
24.5–25	1.042 ± 0.028
26 –28	1.057 ± 0.010
29 –30	1.052 ± 0.005
(Reactor shut-down)	

Table 2
Surface densities of various elements that reduce flux by 1, 5 and 10%*

Element	σ, barns	Surface density (mg/cm²) to give % reduction		
		1%	5%	10%
B	752	0.5	2.5	5
C	$3.4 \cdot 10^{-3}$	$1.2 \cdot 10^{5}$	$5.9 \cdot 10^{5}$	$1.2 \cdot 10^{6}$
Na	$5.3 \cdot 10^{-3}$	$1.5 \cdot 10^{5}$	$7.1 \cdot 10^{5}$	$1.5 \cdot 10^{4}$
Si	0.16	$6.1 \cdot 10^{3}$	$2.9 \cdot 10^{4}$	$6.1 \cdot 10^{4}$
Cl	33.2	37	180	370
Mn	13.3	144	685	$1.4 \cdot 10^{3}$
Fe	2.6	750	$3.6 \cdot 10^{3}$	$7.5 \cdot 10^{3}$
Cd	3620	1.1	5.2	11
Sm	5840	0.9	4.3	9
Gd	$3.91 \cdot 10^{4}$	0.14	0.7	1.4

*Calculated for targets perpendicular to the neutron beam. If placed at an angle Θ, surface densities should be divided by cos Θ.

We studied effects of self absorption that might occur for samples with relatively high concentrations of elements such as B, Cd, Sm and Gd that have very large cross sections. In Table 2 are listed the surface densities that will result in flux

reductions for several important elements commonly observed. These data, which we calculated from thermal neutron cross sections, were confirmed by running standards of several thicknesses for elements with high cross sections.

For each class of samples studied, an initial run was made to determine which elements produced observable lines in the spectrum. The spectra were analyzed by a simple routine that identified and integrated single peaks and multiplets, but did not attempt to resolve the latter. The energy scale was calibrated using lines from N, Fe, Al and Si.[12] The presence of an element was inferred by finding lines attributed to that element in previously published work or our spectra of elemental standards. All "pure" element or compound standards contain impurities of elements with large cross sections, most often Cd, Sm or Gd, whose lines often appear in the standard spectra. Spectra for elements were generally taken using standards made from two or more sources of material in order to identify lines from impurities by variations of their relative intensities. For example, Si standards of ultrapure Si, SiO_2 and semiconductor Si were used. Only those lines that always appeared in the same ratios were attributed to the element under study. Furthermore, since we have detailed spectra of the elements with large cross sections, we are able to observe characteristic patterns of their lines in the standard spectra of other elements and, by normalization to these lines, remove the impurity spectrum from that of the standard.

Once an element's presence had been established in the spectrum of a sample and standards run, it was necessary to establish where interferences existed and measure correction factors for them. An advantage of the complexity of capture γ spectra is that several peaks can usually be used for the analysis of an element and it is not likely that interferences will be present in all of them in a sample. Moreover, well studied interferences can usually be corrected in a reliable manner using one or more large peaks in the spectrum of the interfering element.

In Table 3 we show an analysis of major Ti lines observed in USGS Andesite rock (AGV-1) and in a Ti standard. The intense lines at 1381 and 1762 keV are free of interferences, whereas major corrections would be required to use the other lines for quantitative purposes. A small correction to the 342-keV line is necessary if Sm is present in large quantitites. A detailed list of important lines observable for more than twenty elements, along with interferences, is given in Ref.[13]

With this system, we have explored the analytical capabilities of PGAA by analyzing a wide range of samples. In most crustal samples, e.g., rocks, coal and fly ash, we can measure concentrations of about 17 elements.[10,13] In Table 4, we list energies of γ-rays used in analyses for the more than twenty elements measured in one kind of sample or another, along with the sensitivities of the measurements, detection limits for singles and Compton-suppressed spectra, important interferences and an indication of ease of observation of the elements in coal and rocks. Count

Table 3
Comparison of count rates of Ti peaks in spectra of irradiated andesite rock and Ti standard

E_γ, keV	Count rate (norm. to 341.7 keV line)		Ratio, And./Std.	% of peak from element	Interference	
	Andesite*	Ti standard			Element	E_γ, keV
341.7	1.00	1.00	1.00	100	Sm	342.0
1381.4	1.04	1.03	1.01	99	–	
1586.0	0.132	0.121	1.09	92	Si	1582.0
					Al	1589.7
1761.6	0.546	0.0538	1.01	99	–	–
1792.4	0.0535	0.0248	2.16	46	K	1794.5
					Si	1793.5
4881.3	0.0137	0.0078	1.8	57	K	4869.3 (SE)
					Ca	4878.6 (DE)
5396.0 (DE)	0.0600	0.0441	1.36	73	Ca	5397.9
5737.7 (DE)	0.0624	0.0642	0.97	102	–	–
5907.0 (SE)	0.121	0.0716	1.69	59	Ca	5908.9 (SE)
6248.7	0.140	0.104	1.34	75	Fe	6256.9 (DE)
6418.0	0.126	0.0761	1.66	60	Ca	6419.9
6759.7	0.143	0.110	1.29	77	Fe	6767.9 (SE)
					Cl	6768.0 (DE)
					K	6747.0 (DE)

*USGS rock AGV-1.

rates of lines important in the background have been given elsewhere.[10] Despite large amounts of H, B, Al, etc., in the vicinity of the detection system, backgrounds for most elements are low enough that they do not seriously interfere with the measurements. Also, although we can flush He gas through the beam tube to reduce the N background, we have found that the N background is more constant if we leave air in the tube.

The detection limits listed in Table 4 are based on the Equation:[14]

$$C(\mathrm{mdl}) = 3.29(R_b/t)^{1/2}/S$$

where R_b – background count rate (c/s) under the peak in question; t – counting
t – counting time, (sec);
S – sensitivity for the particular line of the element (net counts/s · mg).

Table 4
Energies, sensitivities, detection limits (singles and suppressed) and interferences for capture γ-rays important for analyses of various elements

Element	E_γ,[a] keV	Sensitivity, c/s/mg	Min. detection limit,[b] mg/g Hawaiian basalt		Interferences[c]	Element measurable in[d]	
			Singles	Comp. suppressed		Coal	Rocks
H	2223	0.86	0.023	0.021		S	M
B	478	530	$6 \cdot 10^{-5}$	$3 \cdot 10^{-5}$	Na, Sm, Gd, Cl, P[e]	S	S
C	1262	$3.9 \cdot 10^{-4}$	22	13	Si, Sm, Gd	M	N
	3684	$1.5 \cdot 10^{-4}$	31	16	N, Si, P, S		
N	1885	0.0030	2.4	1.4	Fe	S	N
	3678	0.0012	3.8	1.9	C		
	5298	0.0017	3.6	–			
F	583	0.0011	10	5	Sm, Cd, F	N	N
	1634D	0.0015	5	3	Cl, V, Sm		
Na	472	0.15	0.09	0.06	B	M	S
	869	0.026	0.40	0.23	K, Sm, Gd		
	1368D	0.036	6	3	Gd		
Mg	585	0.0085	1.4	0.7	F, Sm	N	M
	1809	0.0022	3.6	2.0	P, Cl, Sm		
	2829	0.0020	3.2	1.8	Fe, Cl		
Al	1779D	0.024	0.34	0.19	N, C, Si[f]	S	S
	7213	0.0015	3.1	–	Sm		
Si	1273	0.0036	2.7	1.6	Sm, Gd, K	S	S
	3539	0.0066	0.6	0.3	Fe, P, C, S		
	4933	0.0042	1.5	–	C, Cl		

Table 4 (cont.)

Element	E_γ,[a] keV	Sensitivity, c/s/mg	Min. detection limit,[b] mg/g Hawaiian basalt		Interferences[c]	Element measurable in[d]	
			Singles	Comp. suppressed		Coal	Rocks
P	637	0.0062	1.8	1.0	Cl, Gd	N	W
S	841	0.054	0.19	0.10	K, Sm	S	W
	2380	0.015	0.28	0.17	Cl, Fe		
	3220	0.0067	0.6	0.3	Fe, Ti		
Cl	516	1.4	0.009	0.004	β^+ ann.	S	M
	785+788	1.2	0.013	0.006	Al, Gd, Na		
	1165	1.0	0.009	0.006	Sm, Cd		
K	770	0.13	0.085	0.045	Sm, Gd, S	S	S
	4869SE	0.0028	2.3	–			
Ca	1943	0.022	0.32	0.18	F, Ti, Cl	M	M
Ti	342	0.38	0.045	0.032	Cl, Sm	S	S
	1382	0.38	0.025	0.013	Sm		
V	1434D	0.33	0.022	0.013	Sm, K, Ca, Ti	N	W
Cr	749	0.050	0.22	0.11	Si, Sm	N	W
	835	0.11	0.09	0.05	Na		
Mn	212	0.46	0.07	0.06		W	M
	847D	1.05	0.009	0.004	Gd		
Fe	352	0.046	0.38	0.28	S, Gd, Mn	S	S
	7631+7646	0.013	0.23	–			
Co	277	112	0.017	0.014	Gd, Cu	N	W
Ni	465	0.12	0.12	0.74	Cd, Sm	N	W
Cu	278	0.12	0.17	0.13	Gd	N	N

Zn	1077	0.019	0.44	0.27	Mn, Cu	N	N
Sr	898	0.031	0.33	0.18	Sm, Gd	N	W
	1836	0.028	0.27	0.15	Ti		
Cd	558	170	$7 \cdot 10^{-5}$	$3.5 \cdot 10^{-5}$	Sm, F	M	W
	651	30	$3.5 \cdot 10^{-4}$	$1.8 \cdot 10^{-4}$	Fe		
Ba	627	0.55	0.020	0.010	Gd	N	W
	818	0.0026	1.4	0.72			
Nd	618	0.55	0.020	0.010		M	M
	697	1.3	0.008	0.004	Gd		
Sm	334	640	$3 \cdot 10^{-5}$	$2 \cdot 10^{-5}$	Fe, K, Cl	S	S
	439	320	$4.5 \cdot 10^{-5}$	$3 \cdot 10^{-5}$			
Gd	182	680	$6 \cdot 10^{-5}$	$5 \cdot 10^{-5}$	Dy	S	S
	944	96	$1 \cdot 10^{-4}$	$5 \cdot 10^{-5}$	Cl, Sm, Al		

[a]D indicates line from decay of short or moderate lived radioactivity. SE is single-escape peak.
[b]Assumes 1.5 g sample of Hawaiian Basalt (USGS BHVO-1) observed for 12 hrs.
[c]If not underlined, interference is seldom important enough to require careful subtraction.
[d]S = strong; M = medium strength (observed in most samples); W = weak (rarely observable); N = not detectable
[e]Peak is about 15 keV broad because of Doppler broadening.
[f]Interference from the $^{28}Si(n, p)^{28}Al$ reaction; important only when a large epithermal neutron flux is used.

Note that S is a function of the element, γ-ray, flux and detection system, but not of the sample, so the S values can be determined from elemental standards. By knowing S for the line, one can calculate C (mdl) for that line in the spectrum of any sample based on R_b and t, whether or not the line is observed. Thus, we list C (mdl) values for many elements that are not observed in the rock standard.

Since nearly all peaks listed in Table 4 are FE peaks, S has essentially the same value for singles and Compton-suppressed spectra; however, C (mdl) values are usually lower in the latter because of the reduced background rates under the peaks, R_b. As shown in Table 4, the C (mdl) values for Compton-suppressed spectra are lower than for singles spectra by factors typically from 1.5 to 2. However, one could decrease C (mdl) of the singles mode by removing the NaI(Tℓ) crystal and moving the Ge(Li) detector closer to the sample to increase the sensitivity S for all lines.

Conclusion

A neutron-capture prompt-γ-facility has been designed, installed and evaluated at the National Bureau of Standards reactor. It is a valuable analytical tool capable of analyzing for up to 17 elements in a number of matrices.[10,13] With the use of a beam tube of large diameter, large amounts of hydrogeneous material for thermalization of neutrons, and substantial quantities of B_4C and, to a lesser extent, $^6Li_2CO_3$ and Li_2CO_3 for absorption of neutrons, we have reduced neutron and γ-ray backgrounds sufficiently to observe lines associated with 17 elements in 1 g samples. The detection system is well enough shielded that background levels even for boron, which is used in large amounts to absorb stray neutrons, are low enough that B can be measured down to sub-μg/g levels in 1 g samples. The simultaneous storage of singles, Compton-suppressed and pair spectra from the Ge(Li) detector surrounded by a split-annulus NaI(Tℓ) crystal, permits one to identify the various spectral features with high reliability. Compton suppression reduces the statistical uncertainty of the areas of peaks that are small compared to general spectrum background. Despite the value of this detection system for identifying lines and observing interferences in complex spectra, a properly shielded singles Ge(Li) detector that can be moved closer to the samples is probably superior for routine applications for most elements. The presence of a number of peaks from each element has made possible relatively low uncertainties for the final results as all of these peaks whose ratios with each other are unchanged from the pure element can be used in the analysis. Matrix effects and sample self shielding have been measured and the resultant corrections shown to be small.

*

We thank ROBERT CARTER, JACK STURROCK, JAMES TORRENCE and the operations staff of the NBS reactor for their considerable help on the design, construction and installation of the beam tube. We thank DICK DUFFEY for his continued interest and helpful suggests.

This work was supported in part by the U. S. Department of Energy under Contract No. EY-76S-05-5173. Certain commercial equipment, instruments, or materials are identified in this paper in order to adequately specify the experimental procedure. In no case does such identification imply recommendation or endorsement by the National Bureau of Standards, nor does it imply that the material or equipment identified is necessarily the best available for the purpose.

References

1. T. L. ISENHOUR, G. H. MORRISON, Anal. Chem., 38 (1966) 162.
2. T. L. ISENHOUR, G. H. MORRISON, Anal. Chem., 38 (1966) 167.
3. D. DUFFEY, A. EL-KADY, F. E. SENFTLE, Nucl. Instr. Methods, 80 (1970) 149.
4. R. HENKLEMANN, H. J. BORN, J. Radioanal. Chem., 16 (1973) 473.
5. E. S. GLADNEY, D. B. CURTIS, E. T. JURNEY, Anal. Chim. Acta, 110 (1979) 339.
6. E. S. GLADNEY, D. B. CURTIS, E. T. JURNEY, J. Radioanal. Chem., 46 (1978) 299.
7. E. S. GLADNEY, E. T. JURNEY, D. B. CURTIS, Anal. Chem., 48 (1976) 2139.
8. E. T. JURNEY, D. B. CURTIS, E. S. GLADNEY, Anal. Chem., 49 (1977) 1741..
9. E. S. GLADNEY, A Literature Survey of Chemical Analysis by Thermal Neutron Induced Capture Gamma Ray Spectrometry, Los Alamos Scientific Laboratory Report LA–8028–MS, Sept. 1979.
10. M. P. FAILEY, D. L. ANDERSON, W. H. ZOLLER, G. E. GORDON, R. M. LINDSTROM, Anal. Chem., 51 (1979) 2209.
11. D. J. HUGHES, R. B. SCHWARTZ, Neutron Cross Sections, Brookhaven National Laboratory Report BNL–325, July, 1958.
12. M. L. STELTS, R. E. CHRIEN, Nucl. Instr. Methods, 155 (1978) 253.
13. M. P. FAILEY, Ph. D. Thesis, Department of Chemistry, University of Maryland, 1979.
14. J. M. JAKLEVIC, R. L. WALTER, in X-Ray Fluorescence Analysis of Environmental Samples, T. G. DZUBAY, (Ed.), Ann Arbor Sciences, Ann Arbor, MI, 1977, Ch. 25.